

# Understanding Text-driven Motion Synthesis with Keyframe Collaboration via Diffusion Models

Dong Wei<sup>1\*</sup>, Xiaoning Sun<sup>1\*</sup>, Huaijiang Sun<sup>1</sup>, Bin Li<sup>2</sup>, Shengxiang Hu<sup>1</sup>, Weiqing Li<sup>1</sup>, Jianfeng Lu<sup>1</sup>

<sup>1</sup>Nanjing University of Science and Technology, China

<sup>2</sup>Tianjin AiForward Science and Technology Co., Ltd., China

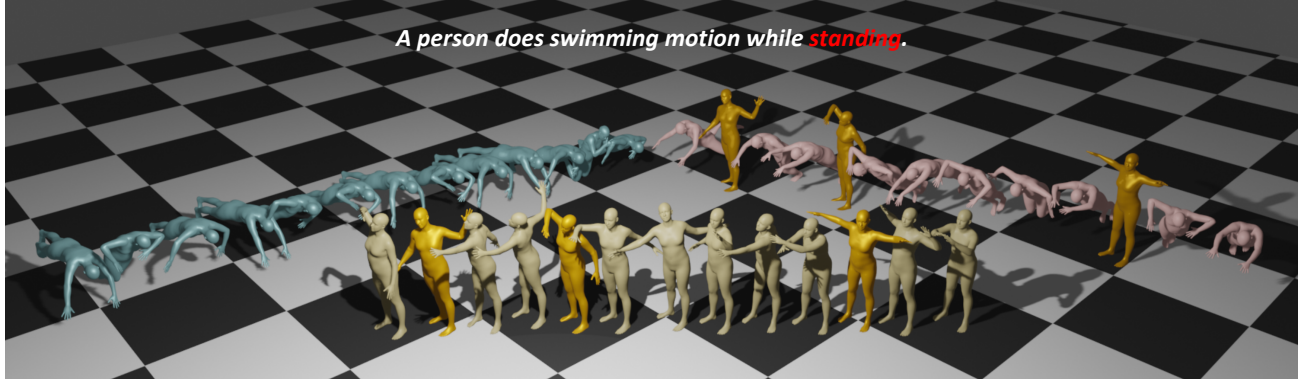


Figure 1: Left: Current text-driven motion diffusion models may misunderstand textual descriptions. Right: Involving keyframe (golden) conditions in diffusion models at *inference* fail to solve this problem. Middle: With keyframes *collaborated*, fine control is allowed, and precise guidance for semantic understanding is provided, leading to correct performance.

## Abstract

The emergence of text-driven motion synthesis technique provides animators with great potential to create efficiently. However, in most cases, textual expressions only contain general and qualitative motion descriptions, while lack fine depiction and sufficient intensity, leading to the synthesized motions that either (a) semantically compliant but uncontrollable over specific pose details, or (b) even deviates from the provided descriptions, bringing animators with undesired cases. In this paper, we propose DiffKFC, a conditional diffusion model for text-driven motion synthesis with keyframes collaborated. Different from plain text-driven designs, full interaction among texts, keyframes and the rest diffused frames are conducted at training, enabling realistic generation under efficient, collaborative dual-level control: coarse guidance at semantic level, with only few keyframes for direct and fine-grained depiction down to body posture level, to satisfy animator requirements without tedious labor. Specifically, we customize efficient Dilated Mask Attention modules, where only partial valid tokens participate in local-to-global attention, indicated by the dilated keyframe

mask. For user flexibility, DiffKFC supports adjustment on importance of fine-grained keyframe control. Experimental results show that our model achieves state-of-the-art performance on text-to-motion datasets HumanML3D and KIT.

## 1. Introduction

Applying human motion synthesis to film or game industries [53] could greatly reduce the dependence on costly motion capture system. To generate animations that meet the needs of animators as well as avoiding them from tedious labor, motion synthesis technique should be able to efficiently generate motions with high fidelity, and with user-friendly interface that allows for flexible and easy control.

As one of the most common information carriers for people, natural language has served as a convenient guidance to provide an overall, coarse control at semantic level. [1, 39, 19] use action labels to produce motions with short lengths and less variations; [17, 18, 40] further use free-form texts with richer descriptions for more complex generation (i.e., text-driven synthesis), under frameworks of GANs [1] or VAEs [39, 18, 40]. Despite great success

achieved, the synthesized motions often suffer from unrealistic behaviors, like drifting or shaky movements.

Recently, denoising diffusion probabilistic models (DDPMs) [48, 21, 49] with high generative quality have alleviated the above problem when applied to text-driven motion synthesis [56, 26, 52, 9]. However, the specific posture details are still uncontrollable for animators, as there would always be various visual needs on synthesized poses that beyond textual descriptions, and it is hard to use texts alone to generate motions towards the desired visual effects while remaining overall semantics.

An alternative way to support fine-grained control is to perform local editing at *inference* stage, which can be defined as an inpainting problem [4, 30]. For instance, MDM [52] regards the first and last frame as constant, and denoises other frames to conduct motion in-betweening. In this context, a natural question arises: *Is getting keyframes involved in inference only while excluded from training, really enough to produce satisfactory results?*

Unfortunately not, due to two reasons: (a) Adding conditional inputs into inference inevitably brings discontinuities, causing great leap between the keyframe and its adjacent frames, to which human eyes are very sensitive. (b) Semantic misunderstanding may happen. For example, given “*a person does swimming motion while standing*”, the model tends to miss the short *standing* word and generates a total *swimming* motion (see Figure 1). If we directly impose keyframe conditions in inference, the discontinuities would become even worse, as the denoising process cannot force every frame towards the correct semantic understanding.

To address above challenges, we propose DiffKFC, a conditional **Diffusion** model for text-driven motion synthesis with **KeyFrames Collaborated**. It prevents animators from the current *dilemma* of either pursuing efficiency by plain text-driven generation while lacking *direct* and *fine-grained* control down to body posture, or pursuing fine motion details by plain keyframe-based generation while requiring dense drawing to achieve desired visual effects. We carefully re-design the vanilla transformer, which fully exploits the internal correlations among tokens of texts, keyframes and the rest diffused parts during training, enabling realistic generations under convenient semantic guidance, only accompanied with few frames of fine depiction to satisfy the requirements of animators.

Considering the reduction of animator labor, our DiffKFC should guarantee the effectiveness of keyframe control even when the provided number is small. Such sparsity of keyframes poses a great challenge to their usage, as the useful keyframe information tends to be overwhelmed when fused with other massive tokens. To this end, we customize efficient Dilated Mask Attention (DMA) modules, which dilate the sparse valid tokens in keyframe mask step by step to “complete” the entire mask to be valid, where the

scope of attention operation expands from local to global, enabling keyframe information to gradually permeate for better fusion with other tokens.

Moreover, for user-friendly concerns, we extend the idea of classifier-free guidance [22], and reserve a variable for users to adjust importance of fine-grained keyframe control under the provided semantic space. Flexible body part editing is also allowed, to re-generate the editing region while remaining consistency and rationality with the fixed, conditional part. Our contributions are as follows:

- We propose a conditional diffusion model for text-driven motion synthesis with keyframes collaborated. A re-designed transformer structure is used for full interaction among multi-modal tokens during training, enabling realistic generation under dual-level control, i.e., convenient semantic guidance, with few keyframes for direct yet fine depiction, towards animator requirements.
- To overcome the challenge brought by the sparsity of keyframes, we customize dilated mask attention modules, which gradually borrow visible useful information from keyframes with local-to-global attention, benefitting its fusion with other tokens.
- Our DiffKFC supports user-friendly variable for adjustment on importance of fine-grained keyframe control under given semantic space, and flexible body part editing. Experiments on text-to-motion datasets HumanML3D and KIT prove its effectiveness.

## 2. Related Work

### 2.1. Human Motion Synthesis

Motion synthesis aims to generate realistic motion sequences based on given conditions. Deep learning enables early methods [24, 23] to generate with parameters of terrain curves or target locations. Later, some controls that can be easily provided by users, such as language and music, have been employed to motion generation using action labels [39, 19] or free-form texts [2, 18, 40], and music-driven dance generation [27, 3, 16], under frameworks of GANs [1], VAEs [39, 18, 40], and with LSTMs [1, 3], GRUs [2, 19], Transformers [39, 27], and graph [16] structures.

**Text-driven motion synthesis** helps animators generate human motions with high efficiency, as motion descriptions contained in free-form texts could control motions towards the target semantics, without tedious labor from animators. Despite the efforts [2, 17, 18, 40], the synthesized motions often suffer from unrealistic behaviors, such as foot sliding and shaky movements. Recently, this problem has been partly alleviated owing to the emergence of motion synthesis with diffusion models [56, 26, 52, 9]. In these works,

texts are encoded by pre-trained CLIP [43], DistilBERT [46] or RoBERTa [29], to be fused with motion embedding with transformer-based [54] architecture, yielding motions of higher generative quality.

Nevertheless, there still remain two unsolved issues: (a) lacking fine control down to body joints under the given semantic space; (b) unable to handle uncertain failures like misunderstanding on textual descriptions. We elaborately incorporate keyframes as direct and fine-grained guidance, which could effectively force motions towards the desired visual effects. Our training with keyframes involved enables its full interaction with texts, and constrains the model to better understand motion descriptions.

## 2.2. Denoising Diffusion Probabilistic Models

Denoising Diffusion Probabilistic Models (DDPMs) [48, 21, 49] is a kind of generative models inspired by particle diffusion process in thermodynamics, and have gained huge popularity recently for their high generative quality. The basic elements of each sample (e.g., pixels of the image, joints of the human body) can be regarded as heated particles that gradually diffuses towards a complete noisy state, and the models will learn its reverse process (i.e., denoising) to recover the data distribution. Success have been achieved in many fields, such as image generation [21, 12, 30], point cloud generation [31, 32] and audio synthesis [27, 3].

**Text-driven motion synthesis with diffusion models** [56, 26, 52] have emerged since the appearance of text-to-image diffusion models [44, 45, 9], where [26, 52] are trained in a classifier-free manner that have no need for an additional classifier structure. [10, 33] propose unified frameworks to deal with both text-driven motion synthesis and music-driven dance generation. [55] designs a motion diffusion model followed with physics-based motion projection module, to eliminate artifacts such as floating.

Notably, diffusion models do support flexible condition setting in inference, without any additional training. However, *analogically* applying this operation to keyframe conditions will inevitably bring obvious discontinuities between the condition part and the generation part. Differently, we involve keyframes in training and use an extra loss term to force the generated transitions to be smooth.

## 2.3. Motion In-filling

Given some discrete specific poses, motion in-filling targets at generating the rest of missing frames, which sometimes is also seen as keyframe-based generation [25, 57, 7, 14, 50, 38]. Along with motion in-betweening that produces intermediate motions based on beginning and last frame(s) [20, 42], and motion prediction that uses past frames to predict future ones [15, 37, 36, 11], they all belong to motion completion, and can be regarded as a branch of motion synthesis. Early motion in-filling is realized by inter-

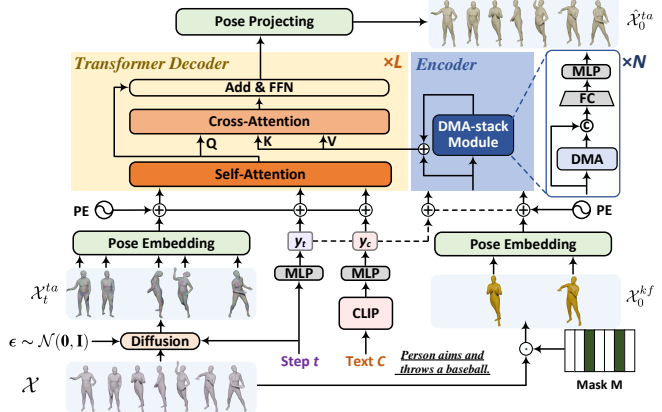


Figure 2: Overview of the proposed DiffKFC method. The encoder of DiffKFC is fed with clean keyframes  $\mathcal{X}_0^{kf}$ , while the decoder of DiffKFC is fed with the rest of frames  $\mathcal{X}_t^{ta}$  in a noising step  $t$  and the output of the encoder. The diffusion step  $t$  and text description  $\mathcal{C}$  are projected to the tokens  $\mathbf{y}_t$  and  $\mathbf{y}_c$ , which are then combined with input tokens. Dilated Mask Attention (DMA) modules are proposed to extract refined tokens from keyframes and texts to conduct better interaction with encoded diffused motion tokens.

polating between adjacent keyframes using linear interpolation (LERP) and spherical linear interpolation (SLERP) [47]. Such method has served as a baseline against (or pre-processing step of) existing deep learning keyframe-based generation models, where convolutional [25, 57, 7], recurrent [20, 50], and transformer [14, 38, 42] structures are employed. GANs are involved to generate more realistic and expressive motions [25, 57, 20]. With CVAEs, [7] proposes a unified framework for different motion synthesis tasks, while [50] realizes generation in real-time.

However, all the above models encounter two problems: (a) limited generative realism; (b) compromise between motion complexity and animator labor, as motions with more details count on dense keyframes. In our work, we are the first to introduce diffusion models into keyframe-related generation task for higher generative quality, and flexible editing property. With collaborative dual-level control, the dependence of complex generation on dense keyframes is broken. Given textual descriptions, with very few drawings at key points, most needs of animations can be achieved.

## 3. Proposed Method

### 3.1. Problem Formulation and Overview

An adapted formulation is given here to suit our task. Existing plain text-driven motion synthesis is aimed at using a free-form textual description, usually a sentence  $\mathcal{C}$ , to generate towards the target  $N$ -frame motion sequence

$\mathcal{X} = \{\mathbf{x}_1, \mathbf{x}_2, \dots, \mathbf{x}_N\}$  with each human pose  $\mathbf{x}_i \in \mathbb{R}^D$  represented by either joint rotations or positions, where  $D = J \times c$ , and  $J$  is the number of joints,  $c$  is the dimension of joint representation. We, additionally, incorporate sparse keyframes  $\mathcal{X}^{kf} = \mathcal{X} \odot \mathbf{M}$  during training, where  $\mathbf{M}$  is a binary mask matrix that preserves keyframe values and zeros the rest of frames (denoted as  $\mathcal{X}^{ta}$ ) to be generated. Note that mask matrix  $\mathbf{M}$  for each sequence could be different.

**Overview of Method.** Our objective is to generate motion conformed to the given text, with keyframes controlled. As shown in Figure 2, we train a *conditional* diffusion model with our re-designed transformer encoder-decoder framework to generate realistic yet controllable human motions. Specifically, a transformer encoder is used to extract refined tokens from keyframes and texts via the proposed Dilated Mask Attention (DMA) modules, followed by full interactions among the text token, the keyframe tokens and the encoded diffused motion tokens (using cross-attention), enriching the representation of each token. The significance of fine-grained keyframes can be adjusted with coarse-grained texts during inference, which enables efficient and convenient dual-level control for animators.

### 3.2. DiffKFC

Our generative model DiffKFC can be described as a latent variable model with the *forward* diffusion process and the *reverse* diffusion process. Intuitively, the diffusion process gradually injects small amount of noise to the data until it is totally transformed to isotropic Gaussian noise, while the reverse process learns to gradually eliminate the noise to recover the original meaningful data.

Unlike existing motion diffusion models [52, 56] that are generally designed for text-to-motion generation, while bluntly involving the first and last pose conditions only during inference for motion in-betweening, our diffusion model, however, has regarded keyframes as an important element for fine-grained control *since training stage*, taking them as a conditional input to fully learn their internal information and exploit their delicate correlations with texts.

**Diffusion Process.** Let  $\mathcal{X}_0^{ta}$  denotes the ground truth sequence ( $N$  human poses) that required to be generated. We define the forward diffusion process as a fixed posterior distribution  $q(\mathcal{X}_{1:T}^{ta} | \mathcal{X}_0^{ta})$ , which can be modeled as a Markov chain according to a fixed variance schedule  $\beta_1, \dots, \beta_T$ :

$$q(\mathcal{X}_t^{ta} | \mathcal{X}_{t-1}^{ta}) = \mathcal{N}(\mathcal{X}_t^{ta}; \sqrt{1 - \beta_t} \mathcal{X}_{t-1}^{ta}, \beta_t \mathbf{I}). \quad (1)$$

A special property is that the diffusion process can be represented in a closed form for any diffusion step  $t$ .

**Reverse Process.** Given a set of specified keyframe  $\mathcal{X}^{kf}$  and a text prompt  $\mathcal{C}$ , we consider the reverse dynamics of the above diffusion process to recover the meaningful sequence  $\mathcal{X}_0^{ta}$  from the white noise  $\mathcal{X}_T^{ta}$ . We formulate this reverse

dynamics with the following parameterization:

$$p_\theta(\mathcal{X}_{t-1}^{ta} | \mathcal{X}_t^{ta}, \mathcal{X}_0^{kf}, \mathcal{C}) = \mathcal{N}(\mathcal{X}_{t-1}^{ta}; \mu_\theta(\mathcal{X}_t^{ta}, \mathcal{X}_0^{kf}, \mathcal{C}, t), \sigma_t^2 \mathbf{I}), \quad (2)$$

where  $\mu_\theta$  is a neural network to estimate the means,  $\sigma_t^2 \mathbf{I}$  is a user-defined variance term of Gaussian transition, and  $\mathcal{X}_0^{kf}$  denotes the clean (not diffused) keyframe matrix.

Previous studies [52, 56] approximate the conditional reverse process Eq.(2) with  $p_\theta(\mathcal{X}_{t-1}^{ta} | \mathcal{X}_t^{ta}, \mathcal{X}_0^{kf}, \mathcal{C})$ , which would harm useful information [51] in the observed keyframes and mislead the text prompt.

**Loss Function.** As revealed in [6], diffusion models can be trained using either the noise prediction [21, 13] or the unnoised data prediction [44, 52]. For the task of motion generation, geometric losses are necessary to constrain the human poses, encouraging coherent and plausible motions. Thus, we directly predict the unnoised data, i.e.,  $\hat{\mathcal{X}}_0^{ta} = f_\theta(\mathcal{X}_t^{ta}, \mathcal{X}_0^{kf}, \mathcal{C}, t)$  instead of  $\epsilon$ -prediction:

$$\mathcal{L}_{simple} = \mathbb{E}_{\mathcal{X}_0^{ta}, t} [\|(\mathcal{X}_0^{ta} - f_\theta(\mathcal{X}_t^{ta}, \mathcal{X}_0^{kf}, \mathcal{C}, t)) \odot (\mathbf{1} - \mathbf{M})\|_2^2], \quad (3)$$

where  $\mathbf{1} - \mathbf{M}$  is a mask that corresponds to  $\mathcal{X}_0^{ta}$ . Similar to [52], we adopt auxiliary kinematic losses  $\mathcal{L}_{phy}$  including joint positions, foot contact and velocities, to enforce physical properties and prevent artifacts like foot sliding. Please refer to supplementary material for details.

In our context, human motion synthesis conditioned on keyframes tends to incur another crucial problem: noticeable discontinuity between generated frames  $\hat{\mathcal{X}}_0^{ta}$  and keyframes  $\mathcal{X}_0^{kf}$ . To address this issue, inspired by [36, 35], we exploit Discrete Cosine Transform (DCT) to strengthen the motion smoothness. We concatenate  $l$  generated frames before and after the  $i$ -th keyframe  $\mathbf{x}_i^{kf}$  to form a new sequence  $\mathbf{G}_i = [\hat{\mathbf{x}}_{i-l}, \dots, \hat{\mathbf{x}}_{i-1}, \mathbf{x}_i^{kf}, \hat{\mathbf{x}}_{i+1}, \dots, \hat{\mathbf{x}}_{i+l}]$ . We remove the high-frequency DCT basis, and approximate this sequence by  $\hat{\mathbf{G}}_i = \mathbf{G}_i \mathbf{D} \mathbf{D}^T$ , where  $\mathbf{D} \in \mathbb{R}^{(2l+1) \times m}$  encodes the first  $m$  DCT bases. Our smoothness loss is defined as:

$$\mathcal{L}_{smooth} = \frac{1}{(2l+1) \cdot K} \sum_{i=1}^K \|\hat{\mathbf{G}}_i - \mathbf{G}_i\|_2^2, \quad (4)$$

where  $K$  denotes the number of keyframes.

Our complete training loss can be formulated as:

$$\mathcal{L} = \lambda_{phy} \mathcal{L}_{phy} + \lambda_{smooth} \mathcal{L}_{smooth} + \mathcal{L}_{simple}. \quad (5)$$

**Inference & Guidance.** According to the inference process in [44, 52], we estimate the clean motion sequence  $\hat{\mathcal{X}}_0^{ta} = f_\theta(\mathcal{X}_t^{ta}, \mathcal{X}_0^{kf}, \mathcal{C}, t)$ , and noise it back to  $\mathcal{X}_{t-1}^{ta}$  until  $T$  times. From animators' perspective, we wish to adjust the importance of fine-grained keyframes  $\mathcal{X}_0^{kf}$  on the motions in line with coarse-grained text description  $\mathcal{C}$ . To this end, we extend the idea of classifier-free guidance [22], which interpolates or extrapolates between the conditioned

model and the unconditioned model. Then, our classifier-free guided inference can be implemented as:

$$f_\theta(\mathcal{X}_t^{ta}, t, \mathcal{C}, \mathcal{X}_0^{kf}) = f_\theta(\mathcal{X}_t^{ta}, t, \mathcal{C}) + s \cdot (f_\theta(\mathcal{X}_t^{ta}, t, \mathcal{C}, \mathcal{X}_0^{kf}) - f_\theta(\mathcal{X}_t^{ta}, t, \mathcal{C})), \quad (6)$$

where  $s$  controls the significance of keyframes in text-driven motion synthesis. For training, our model learns both the dual-level controlled and coarse-grained text only controlled distributions by randomly dropping the keyframe information 10% of the samples, such that  $f_\theta(\mathcal{X}_t^{ta}, \mathcal{C}, t)$  approximates  $p(\mathcal{X}_t^{ta})$ . In practice, this can be achieved by skipping DMA-stack module, i.e., no valid tokens from the encoder are incorporated into cross-attention layers.

### 3.3. Network Architecture

The overall DiffKFC architecture is depicted in Figure 2. We implement the denoising network  $f_\theta$  with a re-designed transformer encoder-decoder structure, as transformer [54] brings two significant property for motion data [39]: capturing global temporal dependencies among human poses, and enabling variable-length motion generation.

**Input Encoding.** Given a keyframe matrix  $\mathcal{X}_0^{kf} \in \mathbb{R}^{D \times N}$  with a mask  $\mathbf{M}$  pointing out which human poses are valid, the rest of missing frames  $\mathcal{X}_0^{ta} = \mathcal{X} \odot (\mathbf{1} - \mathbf{M})$  are gradually incorporated with small noises towards  $\mathcal{X}_T^{ta}$ . We project them into the transformer dimension  $d$  through two separate pose embedding layers, and output  $\mathbf{Y}^{kf}, \mathbf{Y}^{ta} \in \mathbb{R}^{d \times N}$ , each column of which can be regarded as a token. The diffusion step  $t$  and the text  $\mathcal{C}$  are also projected to the corresponding  $d$ -dimension vectors by fully-connected layers, which yields tokens  $\mathbf{y}_t$  and  $\mathbf{y}_c$ . These tokens are then combined with  $\mathbf{Y}^{kf}$  and  $\mathbf{Y}^{ta}$  separately.

**Transformer Body.** Considering that the transformer does not know the order of human poses, the learnable position embedding in ViT [54] is adopted to maintain the positional information of each token. Our **Encoder** is fed with keyframe tokens, along with text token and time token, to extract keyframe information for later use. The **Transformer Decoder** consists of self-attention layers (SA), cross-attention layers (CA) and feed-forward network (FFN). Specifically, it first models strong global correlation between any two tokens (including diffused missing frames in  $\mathcal{X}_T^{ta}$ , text token and diffusion step token) via SA mechanism. Then, it accepts the outputs of the Encoder to exchange the encoded keyframes information by CA layers, and is then fed into FFN. After the fusion with keyframe tokens, missing frame tokens pass the learned information to its own branch, which naturally enriches the representation of each missing frame token. Finally, a linear projection is imposed to recover the transformer dimension  $d$  to pose representations dimension  $D$ . Following DETR [8], our decoder directly outputs the set of human poses in parallel.

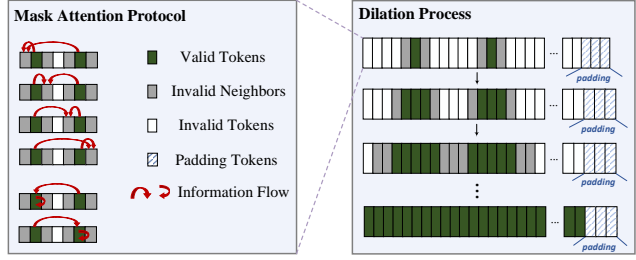


Figure 3: The proposed Dilated Mask Attention (DMA) module. (Left) Mask attention protocol. In the range of valid tokens and their invalid neighbors, the output of attention is computed as the weighted sum of valid tokens while invalid tokens are ignored. (Right) Dilated process. The invalid neighbors are automatically updated to be valid through each attention. After several times of attention and update, the whole sequence becomes fully valid except padding tokens (no benefit to interact with diffused tokens).

However, for our keyframe encoder, we find that directly using ViT encoder fails to borrow visible useful information for inpainting. *This is common as given keyframes are sparse that tends to be overwhelmed when fused into CA layers.* One possible solution is to use SLERP to interpolate keyframes as a pre-processing step, like recent motion in-betweening models [42, 38, 14]. Nevertheless, this lowers the flexibility of keyframe selection, as it requires that at least the first and last frames must be given, and may introduce misleading guidance that harms generative realism and blurs motion details. To tackle the above problem, we carefully design our encoder, to be presented as below.

**Dilated Mask Attention Module.** Inspired by [28] for large hole image inpainting, we propose Dilated Mask Attention (DMA) stack module to handle large number of missing frame tokens (about 95% tokens are invalid). Our key insight is that, since the keyframe matrix contains important yet temporarily unusable information due to sparsity, if we take these visible sparse keyframes as starting points, and find a certain strategy to ‘complete’ the entire sequence, then the ‘completed sequence’ would better interact with the diffused missing frames and texts to generate more natural transitions. That is exactly what our DMA-stack module is designed for, as depicted in Figure 3, to conduct interaction between the valid tokens (green) and their neighbors (grey), so that these neighbors will be gradually contaminated with keyframe information to realize the ‘complete’ process. Recall that the input of our encoder is the concatenation of  $\mathbf{Y}^{kf}$ ,  $\mathbf{y}_t$  and  $\mathbf{y}_c$ , denoted as  $\mathbf{Z} \in \mathbb{R}^{d \times (N+2)}$ . The attention of DMA can be derived by:

$$\text{Att}(\mathbf{Q}, \mathbf{K}, \mathbf{V}) = \text{Softmax}\left(\frac{\mathbf{Q}\mathbf{K}^T + \mathbf{M}'}{\sqrt{d}}\right)\mathbf{V}, \quad (7)$$

where  $\mathbf{Q}$ ,  $\mathbf{K}$ ,  $\mathbf{V}$  are the query, key, value matrices obtained by imposing three learnable linear projections to  $\mathbf{Z}^T$ . The mask  $\mathbf{M}' \in \mathbb{R}^{(N+2) \times (N+2)}$  is defined as:

$$\mathbf{M}'_{ij} = \begin{cases} 0, & \text{if token } j \text{ is valid,} \\ -\infty, & \text{if token } j \text{ is invalid,} \end{cases} \quad (8)$$

where only valid tokens participate in computing weights, while invalid tokens are ignored in current state.

The mask  $\mathbf{M}'$  indicates whether a token is valid, and it is initialized by the input keyframe mask  $\mathbf{M}$ . We design a valid-token-dilation strategy, which automatically activates invalid neighbors to become valid step by step. As illustrated in Figure 3, at every dilation step, attention is conducted between every **(valid token, invalid neighbor)** pair, and therefore dilates the valid region. After several times of such operation, the whole sequence is updated to be fully valid (except padding region). Our dilation on valid regions is a gradual process, which forces the keyframe information to slowly permeate into the entire sequence, with the following two benefits: (a) greatly alleviating the problems caused by keyframe sparsity, which helps to generate more natural and detailed motions; (b) allowing for dilation of attention span from local to global, which helps later full interaction in CA layers with tokens of diffused frames and texts.

In detail, we remove layer normalization to reduce the importance of invalid tokens, and take advantage of feature concatenation to replace residual learning similar to popular diffusion ViT backbone [5]. The input and output of attention are concatenated to feed into a fully-connected layer:

$$\mathbf{Z}'_k = \text{FC}([\text{DMA}(\mathbf{Z}_{k-1}) \parallel \mathbf{Z}_{k-1}]), \quad \mathbf{Z}_k = \text{MLP}(\mathbf{Z}'_k), \quad (9)$$

where  $\mathbf{Z}_k$  is the output of the  $k$ -th DMA block. A global skip connection is adopted to prevent gradient exploding.

### 3.4. Keyframe Picking & Motion Editing

The selection of keyframe positions and numbers is flexible. With our dual-level control, the desired generation can be achieved with textual descriptions and few keyframes, avoiding tedious labor of drawing in exchange for complex motions. Animators may provide more keyframes if they wish, at key points, or over undescribable details.

Unlike introducing keyframe conditions *only* during inference, body part editing *only* during inference, however, is allowed, which denoises the editing part [4, 52] as well as maintaining consistency with the conditional body part. The difference lies in that, the discontinuity in temporal domain will cause noticeable leap between frames to which human eyes are very sensitive, but in spatial domain, causes only a small range of deviations on certain joint positions, and therefore are totally acceptable. Given a subset of sequences  $\mathcal{X}^{\text{ref}} = \mathcal{X} \odot \mathbf{M}^{\text{ref}}$ , with  $\mathbf{M}^{\text{ref}}$  indicating which body part serves as condition, we overwrite the outputs  $\hat{\mathcal{X}}_0^{\text{ta}}$

of our model with  $\mathcal{X}^{\text{ref}}$  at each denoising step. In this way, body parts can be generated according to text prompt and keyframes while  $\mathcal{X}^{\text{ref}}$  remains unchanged. Actually, in this case, animators are only required to draw editable body parts of keyframes, i.e.,  $(\mathcal{X} \odot \mathbf{M}) \odot (\mathbf{1} - \mathbf{M}^{\text{ref}})$ .

## 4. Experiments

In this section, to evaluate our proposed model, we introduce two datasets, evaluation metrics, implementation details, and comparable baselines. Results, visualizations and analyses are followed. We also provide ablation study to show the impact of each component.

### 4.1. Datasets

**KIT Motion-Language dataset** [41] is a text-to-motion dataset that contains 3,911 human motion sequences and 6,353 sentences of textual descriptions. Dataset split procedure is consistent with prior [2, 40, 26].

**HumanML3D** [18] is a newly published dataset that annotates existing 3D motion capture datasets AMASS [34] and HumanAct12 [19], containing 14,616 motions with 44,970 textual descriptions. Each frame is represented by the concatenation of root velocities, joint positions, joint velocities joint rotations, and foot contact labels. We follow [18, 52] to use this representation as well as on KIT dataset.

### 4.2. Evaluation Metrics & Baselines

**Evaluation Metrics.** In accordance with [18, 56, 52], we use five metrics provided by [18]. (1) *Frechet Inception Distance (FID)*: similarity between the distribution of generations and ground truth; (2) *R-Precision*: the alignment between the generation and the text, which is obtained by drawing the GT description of each generated sequence with 31 mismatched descriptions into a description pool, ranking Euclidean distances between the generation and each description within the pool, and picking top-3 average motion-retrieval accuracies; (3) *Diversity*: the average joint differences between each pairs of generated motions that are randomly split; (4) *MultiModality*: the diversity between each generated motions under the same semantic space; (5) *MultiModality Distance (MM Dist)*: the average Euclidean distance between features of each generated motion and corresponding description.

**Baselines.** We choose two groups of baselines. Group A: Text-to-motion synthesis models JL2P [2], Hier [17], TEMOS [40] and T2M [18], with the former two aimed at generating single motion sequence while the latter two aimed at multiple ones. Group B: The newly proposed diffusion models on text-driven motion synthesis MDM [52] and MoFusion [10].

Method	R-Precision $\uparrow$			FID $\downarrow$	MM Dist $\downarrow$	Diversity $\rightarrow$	MultiModality $\downarrow$
	Top 1	Top 2	Top 3				
Real motion	0.511 $\pm$ .003	0.703 $\pm$ .003	0.797 $\pm$ .002	0.002 $\pm$ .000	2.974 $\pm$ .008	9.503 $\pm$ .065	-
JL2P [2]	0.246 $\pm$ .001	0.387 $\pm$ .002	0.486 $\pm$ .002	11.02 $\pm$ .046	5.296 $\pm$ .008	7.676 $\pm$ .058	-
Hier [17]	0.301 $\pm$ .002	0.425 $\pm$ .002	0.552 $\pm$ .004	6.532 $\pm$ .024	5.012 $\pm$ .018	8.332 $\pm$ .042	-
TEMOS [40]	0.424 $\pm$ .002	0.612 $\pm$ .002	0.722 $\pm$ .002	3.734 $\pm$ .028	3.703 $\pm$ .008	8.973 $\pm$ .071	0.368 $\pm$ .018
T2M [18]	<b>0.457<math>\pm</math>.002</b>	<b>0.639<math>\pm</math>.003</b>	<b>0.740<math>\pm</math>.003</b>	1.067 $\pm$ .002	<b>3.340<math>\pm</math>.008</b>	9.188 $\pm$ .002	2.090 $\pm$ .083
MDM [52]	0.320 $\pm$ .005	0.498 $\pm$ .004	0.611 $\pm$ .007	0.544 $\pm$ .044	5.566 $\pm$ .027	9.559 $\pm$ .086	2.799 $\pm$ .072
MoFusion [10]	-	-	0.492	-	-	8.82	2.52
DiffKFC	<u>0.380<math>\pm</math>.005</u>	<u>0.570<math>\pm</math>.005</u>	<u>0.681<math>\pm</math>.005</u>	<b>0.148<math>\pm</math>.029</b>	<u>4.988<math>\pm</math>.022</u>	<b>9.467<math>\pm</math>.087</b>	<b>0.288<math>\pm</math>.021</b>

Table 1: Results of two groups of baselines and DiffKFC on HumanML3D dataset.  $\rightarrow$  means results are better when closer to that of real motion.  $\uparrow$  means previous works pursuing higher values while ours pursuing lower. We evaluate with 5 times of running for MultiModality while 20 times for other metrics, under 95% confidence interval. **Bold** indicates best results; underline indicates best results under diffusion setting; “-” means unavailable results.

Method	R-Precision (Top 3) $\uparrow$	FID $\downarrow$	MM Dist $\downarrow$	Diversity $\rightarrow$	Multi- Modality $\downarrow$
JL2P [2]	0.483 $\pm$ .005	6.545 $\pm$ .072	5.147 $\pm$ .030	9.073 $\pm$ .100	-
Hier [17]	0.531 $\pm$ .007	5.203 $\pm$ .107	4.986 $\pm$ .027	9.563 $\pm$ .072	-
TEMOS [40]	0.687 $\pm$ .005	3.717 $\pm$ .051	3.417 $\pm$ .019	10.84 $\pm$ .100	0.532 $\pm$ .034
T2M [18]	<b>0.693<math>\pm</math>.007</b>	2.770 $\pm$ .109	<b>3.401<math>\pm</math>.008</b>	10.91 $\pm$ .119	1.482 $\pm$ .065
MDM [52]	0.396 $\pm$ .004	0.497 $\pm$ .021	9.191 $\pm$ .022	10.85 $\pm$ .109	1.907 $\pm$ .214
DiffKFC	<u>0.414<math>\pm</math>.006</u>	<b>0.180<math>\pm</math>.028</b>	<u>8.908<math>\pm</math>.012</u>	<b>10.97<math>\pm</math>.112</b>	<b>0.196<math>\pm</math>.052</b>

Table 2: Results of baselines and DiffKFC on KIT dataset.

### 4.3. Implementation Details

As for the diffusion model, the number of diffusion steps  $t$  is 1,000 with cosine beta scheduling following [52, 26]. We employ an off-the-shelf CLIP [43] to encode the text prompt  $\mathcal{C}$ . For each motion sequence, we randomly select 5% keyframes for fine-grained control, which is much less than that of motion in-between methods [38, 20]. The encoder of our DiffKFC has 8 layers, and their dilated step size (the number of invalid neighbors of each valid token) is set to  $\{2, 2, 4, 4, 6, 6, 8, N\}$ . As for the decoder, we build up 8 transformer layers with 8 heads, latent dimension  $d = 512$  and feed-forward size 1,024. Our model is trained with batch size 64 for 500K steps on the HumanML3D and 200K steps on the KIT dataset. The guidance scale  $s$  of DiffKFC is set as 2.5 during inference. According to [52, 18], we do not use geometric losses for HumanML3D dataset since foot contact and joint locations are explicitly represented.

### 4.4. Results

FID value is lowest in DiffKFC, indicating the best generative quality, where our generated feature distributions are the closest to real motion on both datasets (see Table 1, 2), as keyframes can provide more direct and fine control that restrains the generation towards the real (desired) scenario.

**R-Precision & MultiModality Distance** reflect the text-motion matching extent. Our model fails to achieve the most advanced results, nor do other diffusion models. However, DiffKFC does significantly outperform Group C, which also verifies the effectiveness of keyframe collaboration under diffusion setting, due to the direct control and precise for semantic understanding provided by keyframes. User study and visualization in our supplementary material could further prove that worse results on this two metrics do not represent low text-motion matching visual effects.

**Diversity** in ours is closer to that of real motions, which indicates that our generations resemble human real behaviors, and are more in line with the natural law.

**MultiModality** in previous multi-generation models is expected to be the higher the better, as they are supposed to generate multiple possible yet diverse motions under each textual description. Our model yields the lowest, but it is exactly what we expect. With the constrain of keyframes, the generative space would be greatly narrowed down, which means that *all the possible generations point towards the expectation of the animator*, so that DiffKFC would be more likely to generate the exact desired results within the narrowed space. We further provide MultiModality changing under different setting of keyframe number in Sec 4.5.

Two visualized cases are in Figure 4 left and middle, showing the comparison between MDM and ours. The top figure in each case either (a) be semantically compliant but inconsistent with desired visual effects, or (b) misunderstands the descriptions, which are all solved in ours. Motion editing case is in Figure 4 right, where certain body part can be edited under given texts and fine-grained key-part (i.e., certain part of the keyframe), while remaining consistency with the fixed, conditional part. Notably, darker colors indicate later occurrence. Additional qualitative and quantitative analyses may refer to our supplementary material.

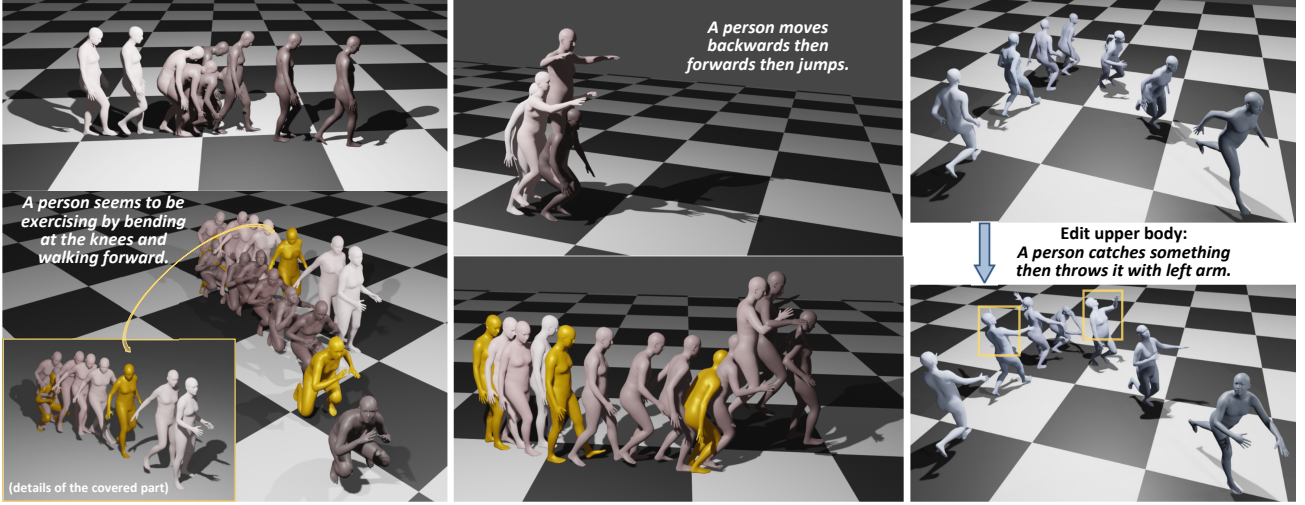


Figure 4: Left & Middle: Visualizations of MDM (top) and ours (bottom). Left: The description is ambiguous on whether “bending *then* walking” or “bending *while* walking”, so both results are semantically reasonable; but with keyframes (yellow) guided, this ambiguity is removed. Middle: Semantic misunderstanding in MDM is corrected in ours. Right: Body part editing, where upper body is edited by the guidance of texts and key-part (upper part of keyframe, marked in yellow boxes).

#### 4.5. Ablation Study

**Discuss on keyframe encoding.** In DiffKFC, keyframe conditions and diffused missing frames are separately encoded, with DMA-stack structure. A common design of conditional diffusion model is to directly concatenate the condition part and the diffused missing part, which are then together fed into a unified encoder (i.e., Unified Enc.); Meanwhile, to validate the effectiveness of DMA-stack structure, we substitute our Encoder with a vanilla transformer encoder (i.e., Vanilla Enc.). Results of this two designing are shown in Table 3.

For the first row, the unified encoding of condition parts and diffused parts makes it hard to distinguish between keyframe and noised targets, which may harm the useful keyframe information, leading to unsatisfactory results. For the second row where the information of sparse keyframes is overwhelmed when fused into CA layers, the results are also worse, indicating that our dilation strategy is valid.

Method	R-Precision (Top 3) $\uparrow$	FID $\downarrow$	MM Dist $\downarrow$	Diversity $\rightarrow 9.503 \pm .065$	Multi- Modality $\downarrow$
Unified Enc.	$0.655 \pm .005$	$0.293 \pm .032$	$5.222 \pm .023$	$9.150 \pm .104$	$0.397 \pm .066$
Vanilla Enc.	$0.498 \pm .010$	$1.118 \pm .096$	$5.879 \pm .073$	$8.921 \pm .049$	$0.581 \pm .054$
DiffKFC	$0.681 \pm .005$	$0.148 \pm .029$	$4.988 \pm .022$	$9.467 \pm .087$	$0.288 \pm .021$

Table 3: Results of Unified Encoder, Vanilla Encoder and DiffKFC on HumanML3D. Our design yields the best.

**Discuss on keyframe rate.** Compared to our keyframe number 5% of the total frames, we further set it to 10%, 2.5% and 0%, respectively, to evaluate their impacts. In Ta-

ble 4, results of 0% keyframe deteriorate significantly (i.e., plain text-driven). However, when keyframes are involved, results of every setting all get improved. Although the more keyframes the better the results, it still proves that only few keyframes are sufficient to help yield satisfactory performance, which shows the valid usage of sparse keyframes, and more importantly, allows reduction on the dependence of dense drawing by animators in real-world scenarios.

Keyframe rate	R-Precision (Top 3) $\uparrow$	FID $\downarrow$	MM Dist $\downarrow$	Diversity $\rightarrow 9.503 \pm .065$	Multi- Modality $\downarrow$
10%	$0.691 \pm .010$	$0.140 \pm .018$	$4.582 \pm .031$	$9.474 \pm .098$	$0.121 \pm .024$
5%	$0.681 \pm .005$	$0.148 \pm .029$	$4.988 \pm .022$	$9.467 \pm .087$	$0.288 \pm .021$
2.5%	$0.663 \pm .007$	$0.291 \pm .021$	$5.310 \pm .028$	$9.595 \pm .073$	$0.895 \pm .021$
0%	$0.602 \pm .008$	$0.597 \pm .025$	$5.721 \pm .036$	$9.576 \pm .049$	$2.984 \pm .054$

Table 4: Comparison among DiffKFC with different keyframe rates on HumanML3D dataset.

#### 5. Conclusion

In this paper, we propose DiffKFC, a conditional diffusion model for text-driven motion synthesis with keyframes collaborated. We carefully re-design a transformer structure for full interaction among multi-modal tokens during training, to realize realistic yet efficient generation under semantic guidance along with direct and fine-grained control by few keyframes. We customize dilated mask attention modules that gradually borrow visible useful information with local-to global attention for more effective fusion with other information, overcoming the challenge caused by keyframe

sparsity. Our model is user-friendly for flexible keyframe selection, body part editing, and adjustment on keyframe importance under given semantic space. Experimental results on HumanML3D and KIT datasets demonstrate the superior performance of our proposed DiffKFC.

**Limitation.** The inference speed of our DiffKFC is slightly lower than SoTA models due to the encodings of keyframes and about 1,000 reverse steps. Future work could speed up the model with fundamental advances in diffusion models.

## References

- [1] Hyemin Ahn, Timothy Ha, Yunho Choi, Hwiyeon Yoo, and Songhwai Oh. Text2action: Generative adversarial synthesis from language to action. In *ICRA*, pages 5915–5920, 2018. [1, 2](#)
- [2] Chaitanya Ahuja and Louis-Philippe Morency. Language2pose: Natural language grounded pose forecasting. In *3DV*, pages 719–728. IEEE, 2019. [2, 6, 7](#)
- [3] Andreas Aristidou, Anastasios Yiannakidis, Kfir Aberman, Daniel Cohen-Or, Ariel Shamir, and Yiorgos Chrysanthou. Rhythm is a dancer: Music-driven motion synthesis with global structure. *TVCG*, 2022. [2, 3](#)
- [4] Omri Avrahami, Dani Lischinski, and Ohad Fried. Blended diffusion for text-driven editing of natural images. In *CVPR*, pages 18208–18218, 2022. [2, 6](#)
- [5] Fan Bao, Chongxuan Li, Yue Cao, and Jun Zhu. All are worth words: a vit backbone for score-based diffusion models. *arXiv preprint arXiv:2209.12152*, 2022. [6](#)
- [6] Yaniv Benny and Lior Wolf. Dynamic dual-output diffusion models. In *CVPR*, pages 11482–11491, 2022. [4](#)
- [7] Yujun Cai, Yiwei Wang, Yiheng Zhu, Tat-Jen Cham, Jianfei Cai, Junsong Yuan, Jun Liu, Chuanxia Zheng, Sijie Yan, Henghui Ding, et al. A unified 3d human motion synthesis model via conditional variational auto-encoder. In *ICCV*, pages 11645–11655, 2021. [3](#)
- [8] Nicolas Carion, Francisco Massa, Gabriel Synnaeve, Nicolas Usunier, Alexander Kirillov, and Sergey Zagoruyko. End-to-end object detection with transformers. In *ECCV*, pages 213–229. Springer, 2020. [5](#)
- [9] Xin Chen, Biao Jiang, Wen Liu, Zilong Huang, Bin Fu, Tao Chen, Jingyi Yu, and Gang Yu. Executing your commands via motion diffusion in latent space. *arXiv preprint arXiv:2212.04048*, 2022. [2, 3](#)
- [10] Rishabh Dabral, Muhammad Hamza Mughal, Vladislav Golyanik, and Christian Theobalt. Mofusion: A framework for denoising-diffusion-based motion synthesis. *CVPR*, 2023. [3, 6, 7](#)
- [11] Lingwei Dang, Yongwei Nie, Chengjiang Long, Qing Zhang, and Guiqing Li. Msr-gcn: Multi-scale residual graph convolution networks for human motion prediction. In *ICCV*, pages 11467–11476, 2021. [3](#)
- [12] Prafulla Dhariwal and Alexander Nichol. Diffusion models beat gans on image synthesis. *NeurIPS*, 34:8780–8794, 2021. [3](#)
- [13] Prafulla Dhariwal and Alexander Nichol. Diffusion models beat gans on image synthesis. *NeurIPS*, 34:8780–8794, 2021. [4](#)
- [14] Yinglin Duan, Yue Lin, Zhengxia Zou, Yi Yuan, Zhehui Qian, and Bohan Zhang. A unified framework for real time motion completion. In *AAAI*, volume 36, pages 4459–4467, 2022. [3, 5](#)
- [15] Katerina Fragkiadaki, Sergey Levine, Panna Felsen, and Jitendra Malik. Recurrent network models for human dynamics. In *ICCV*, pages 4346–4354, 2015. [3](#)
- [16] Jibin Gao, Junfu Pu, Honglun Zhang, Ying Shan, and Wei-Shi Zheng. Pc-dance: Posture-controllable music-driven dance synthesis. In *ACM MM*, pages 1261–1269, 2022. [2](#)
- [17] Anindita Ghosh, Noshaba Cheema, Cennet Oguz, Christian Theobalt, and Philipp Slusallek. Synthesis of compositional animations from textual descriptions. In *ICCV*, pages 1396–1406, 2021. [1, 2, 6, 7](#)
- [18] Chuan Guo, Shihao Zou, Xinxin Zuo, Sen Wang, Wei Ji, Xingyu Li, and Li Cheng. Generating diverse and natural 3d human motions from text. In *CVPR*, pages 5152–5161, 2022. [1, 2, 6, 7](#)
- [19] Chuan Guo, Xinxin Zuo, Sen Wang, Shihao Zou, Qingyao Sun, Annan Deng, Minglun Gong, and Li Cheng. Action2motion: Conditioned generation of 3d human motions. In *ACM MM*, pages 2021–2029, 2020. [1, 2, 6](#)
- [20] Félix G Harvey, Mike Yurick, Derek Nowrouzezahrai, and Christopher Pal. Robust motion in-betweening. *TOG*, 39(4):60–1, 2020. [3, 7](#)
- [21] Jonathan Ho, Ajay Jain, and Pieter Abbeel. Denoising diffusion probabilistic models. *NeurIPS*, 33:6840–6851, 2020. [2, 3, 4](#)
- [22] Jonathan Ho and Tim Salimans. Classifier-free diffusion guidance. *arXiv preprint arXiv:2207.12598*, 2022. [2, 4](#)
- [23] Daniel Holden, Taku Komura, and Jun Saito. Phase-functioned neural networks for character control. *TOG*, 36(4):1–13, 2017. [2](#)
- [24] Daniel Holden, Jun Saito, and Taku Komura. A deep learning framework for character motion synthesis and editing. *TOG*, 35(4):1–11, 2016. [2](#)
- [25] Manuel Kaufmann, Emre Aksan, Jie Song, Fabrizio Pece, Remo Ziegler, and Otmar Hilliges. Convolutional autoencoders for human motion infilling. In *3DV*, pages 918–927. IEEE, 2020. [3](#)
- [26] Jihoon Kim, Jiseob Kim, and Sungjoon Choi. Flame: Free-form language-based motion synthesis & editing. In *AAAI*, 2023. [2, 3, 6, 7](#)
- [27] Rui long Li, Shan Yang, David A Ross, and Angjoo Kanazawa. Ai choreographer: Music conditioned 3d dance generation with aist++. In *ICCV*, pages 13401–13412, 2021. [2, 3](#)
- [28] Wenbo Li, Zhe Lin, Kun Zhou, Lu Qi, Yi Wang, and Jiaya Jia. Mat: Mask-aware transformer for large hole image inpainting. In *CVPR*, pages 10758–10768, 2022. [5](#)
- [29] Yinhan Liu, Myle Ott, Naman Goyal, Jingfei Du, Mandar Joshi, Danqi Chen, Omer Levy, Mike Lewis, Luke Zettlemoyer, and Veselin Stoyanov. Roberta: A robustly optimized bert pretraining approach. *arXiv preprint arXiv:1907.11692*, 2019. [3](#)
- [30] Andreas Lugmayr, Martin Danelljan, Andres Romero, Fisher Yu, Radu Timofte, and Luc Van Gool. Repaint: Inpainting

using denoising diffusion probabilistic models. In *CVPR*, pages 11461–11471, 2022. 2, 3

[31] Shitong Luo and Wei Hu. Diffusion probabilistic models for 3d point cloud generation. In *CVPR*, pages 2837–2845, 2021. 3

[32] Zhaoyang Lyu, Zhifeng Kong, XU Xudong, Liang Pan, and Dahua Lin. A conditional point diffusion-refinement paradigm for 3d point cloud completion. In *ICLR*, 2022. 3

[33] Jianxin Ma, Shuai Bai, and Chang Zhou. Pretrained diffusion models for unified human motion synthesis. *arXiv preprint arXiv:2212.02837*, 2022. 3

[34] Naureen Mahmood, Nima Ghorbani, Nikolaus F Troje, Gerard Pons-Moll, and Michael J Black. Amass: Archive of motion capture as surface shapes. In *ICCV*, pages 5442–5451, 2019. 6

[35] Wei Mao, Miaomiao Liu, and Mathieu Salzmann. Weakly-supervised action transition learning for stochastic human motion prediction. In *CVPR*, pages 8151–8160, 2022. 4

[36] Wei Mao, Miaomiao Liu, Mathieu Salzmann, and Hongdong Li. Learning trajectory dependencies for human motion prediction. In *ICCV*, pages 9489–9497, 2019. 3, 4

[37] Julieta Martinez, Michael J Black, and Javier Romero. On human motion prediction using recurrent neural networks. In *CVPR*, pages 2891–2900, 2017. 3

[38] Boris N Oreshkin, Antonios Valkanas, Félix G Harvey, Louis-Simon Ménard, Florent Bocquelet, and Mark J Coates. Motion inbetweening via deep  $\Delta$ -interpolator. *arXiv preprint arXiv:2201.06701*, 2022. 3, 5, 7

[39] Mathis Petrovich, Michael J Black, and Güл Varol. Action-conditioned 3d human motion synthesis with transformer vae. In *ICCV*, pages 10985–10995, 2021. 1, 2, 5

[40] Mathis Petrovich, Michael J Black, and Güл Varol. Temos: Generating diverse human motions from textual descriptions. In *ECCV*, pages 480–497. Springer, 2022. 1, 2, 6, 7

[41] Matthias Plappert, Christian Mandery, and Tamim Asfour. The kit motion-language dataset. *Big data*, 4(4):236–252, 2016. 6

[42] Jia Qin, Youyi Zheng, and Kun Zhou. Motion in-betweening via two-stage transformers. *TOG*, 41(6):1–16, 2022. 3, 5

[43] Alec Radford, Jong Wook Kim, Chris Hallacy, Aditya Ramesh, Gabriel Goh, Sandhini Agarwal, Girish Sastry, Amanda Askell, Pamela Mishkin, Jack Clark, et al. Learning transferable visual models from natural language supervision. In *ICML*, pages 8748–8763. PMLR, 2021. 3, 7

[44] Aditya Ramesh, Prafulla Dhariwal, Alex Nichol, Casey Chu, and Mark Chen. Hierarchical text-conditional image generation with clip latents. *arXiv preprint arXiv:2204.06125*, 2022. 3, 4

[45] Chitwan Saharia, William Chan, Saurabh Saxena, Lala Li, Jay Whang, Emily Denton, Seyed Kamyar Seyed Ghasemipour, Burcu Karagol Ayan, S Sara Mahdavi, Rapha Gontijo Lopes, et al. Photorealistic text-to-image diffusion models with deep language understanding. *NeurIPS*, 2022. 3

[46] Victor Sanh, Lysandre Debut, Julien Chaumond, and Thomas Wolf. Distilbert, a distilled version of bert: smaller, faster, cheaper and lighter. *arXiv preprint arXiv:1910.01108*, 2019. 3

[47] Ken Shoemake. Animating rotation with quaternion curves. In *SIGGRAPH*, pages 245–254, 1985. 3

[48] Jascha Sohl-Dickstein, Eric Weiss, Niru Maheswaranathan, and Surya Ganguli. Deep unsupervised learning using nonequilibrium thermodynamics. In *ICML*, pages 2256–2265. PMLR, 2015. 2, 3

[49] Yang Song and Stefano Ermon. Scorebased generative modeling through stochastic differential equations. *ICLR*, 2021. 2, 3

[50] Xiangjun Tang, He Wang, Bo Hu, Xu Gong, Ruifan Yi, Qilong Kou, and Xiaogang Jin. Real-time controllable motion transition for characters. *TOG*, 41(4):1–10, 2022. 3

[51] Yusuke Tashiro, Jiaming Song, Yang Song, and Stefano Ermon. Csd: Conditional score-based diffusion models for probabilistic time series imputation. *NeurIPS*, 34:24804–24816, 2021. 4

[52] Guy Tevet, Sigal Raab, Brian Gordon, Yonatan Shafir, Daniel Cohen-Or, and Amit H Bermano. Human motion diffusion model. *ICLR*, 2023. 2, 3, 4, 6, 7

[53] Herwin Van Welbergen, Ben JH Van Basten, Arjan Egges, Zs M Ruttkay, and Mark H Overmars. Real time animation of virtual humans: a trade-off between naturalness and control. In *Computer Graphics Forum*, pages 2530–2554, 2010. 1

[54] Ashish Vaswani, Noam Shazeer, Niki Parmar, Jakob Uszkoreit, Llion Jones, Aidan N Gomez, Łukasz Kaiser, and Illia Polosukhin. Attention is all you need. *NeurIPS*, 30, 2017. 3, 5

[55] Ye Yuan, Jiaming Song, Umar Iqbal, Arash Vahdat, and Jan Kautz. Physdiff: Physics-guided human motion diffusion model. *arXiv preprint arXiv:2212.02500*, 2022. 3

[56] Mingyuan Zhang, Zhongang Cai, Liang Pan, Fangzhou Hong, Xinying Guo, Lei Yang, and Ziwei Liu. Motondiffuse: Text-driven human motion generation with diffusion model. *arXiv preprint arXiv:2208.15001*, 2022. 2, 3, 4, 6

[57] Yi Zhou, Jingwan Lu, Connelly Barnes, Jimei Yang, Sitao Xiang, et al. Generative tweening: Long-term inbetweening of 3d human motions. *arXiv preprint arXiv:2005.08891*, 2020. 3